Virology 526 (2019) 61–71

Contents lists available at ScienceDirect

Virology

journal homepage: www.elsevier.com/locate/virology

Bombyx mori nucleopolyhedrovirus F-like protein Bm14 affects the morphogenesis and production of occlusion bodies and the embedding of ODVs

Weifan Xu, Ying Fan, Haiping Wang, Min Feng, Xiaofeng Wu*

College of Animal Science, Zhejiang University, Hangzhou 310058, Zhejiang, China

ARTICLE INFO

Keywords:
BmNPV
F-like protein
OB
ODV occlusion

ABSTRACT

In group I nucleopolyhedrovirus such as Bombyx mori nucleopolyhedrovirus (BmNPV), the biological functions of F-like protein (Bm14) still remain elusive. Here, we found that the deletion of *Bm14* reduced the production rate of infectious budded viruses in cell culture, delayed the lethal time of infected larvae by approximately 26 h, and produced less occlusion bodies (OBs). Scanning electron microscopy demonstrated that its disruption affected OB morphogenesis, forming irregular OBs with a pitted surface and irregular profiles. Moreover, almost 45% less DNA was present in OBs produced by *Bm14*-null virus. This reduction in DNA content was consistent with fewer virions embedded into OBs. The titers of occlusion-derived viruses was 7.5 times less in mutant OBs. Western blot analysis revealed that Bm14 is present in the envelope of both BV and ODV. Taken together, Bm14 is a viral factor that affects OB morphogenesis and production, and the number of ODVs occluded into OBs.

1. Introduction

Baculoviruses (*Baculoviridae*) represent a large group of enveloped double-stranded DNA viruses with rod-shape and a limited host range within insects, particularly Lepidoptera, Hymenoptera, and Diptera (Blissard et al., 2002; Blissard and Theilmann, 2018; Moscardi, 1999; Rohrmann, 2011). The family *Baculoviridae* currently contains four genera: *Alphabaculovirus*, *Betabaculovirus*, *Gammabaculovirus*, and *Deltabaculovirus* (Jehle et al., 2006). Phylogenetic studies further indicate that *Alphabaculovirus* can be subdivided into two subgroups, groups I and II (Carstens, 2011; Cory and Myers, 2003; Herniou et al., 2001). More interestingly, baculoviruses have developed a unique biphasic infection cycle which produces two different phenotypes of virions, the budded virus (BV) and the occlusion-derived virus (ODV). BVs are capable of infecting most cell types within the susceptible hosts and thus responsible for systemic virions spreading, while ODVs are in charge of the infection of larval arthropods and mediate the transmission of viral infection from host to host.

It is generally known that the entry of enveloped viruses into host cells is mediated by viral envelope proteins (Plemper, 2011). In baculoviruses, BVs appear to have two major envelope proteins, GP64 and F protein. Although they are reported to play similar biological roles in virus entry and egress, they performed in different patterns of action (Hefferon et al., 1999a; Kadlec et al., 2008b; Kingsley et al., 1999; Wang et al., 2014, 2010a; Westenberg et al., 2007, 2002; Wfj et al., 2000; Yin et al., 2013). As the major glycoprotein found in group I NPVs, GP64 is required for binding to the cell surface receptors during the process of viral entry by receptor mediated endocytosis (Hefferon et al., 1999b; Kataoka et al., 2012; Westenberg et al., 2007; Zhou and Blissard, 2008). Once the virions are in the endosome, GP64 also mediates low-pH dependent membrane fusion between the viral envelope and endosome membrane, and thus lead to the release of the nucleocapsids into the cytoplasmic (Blissard and Wenz, 1992a, 1992b; Kadlec et al., 2008a; Katou et al., 2010; Li and Blissard, 2009). In addition, GP64 is also essential for nucleocapsid budding from the cell surface (Haines et al., 2009; Li and Blissard, 2010; Oomens and Blissard, 1999). Functionally analogous to GP64, F proteins in group II NPVs show no sequence similarity to GP64 but also possess pH-triggered membrane fusion activity via a conserved proprotein convertase (furin-like) cleavage site (Lung et al., 2002; Westenberg et al., 2002).

Abbreviations: NPV, nucleopolyhedrovirus; BmNPV, Bombyx mori nucleopolyhedrovirus; AcMNPV, Autographa californica multiple nucleopolyhedrovirus; OpMNPV, Orgyia pseudotsugata multiple nucleopolyhedrovirus; HearNPV, Helicoverpa armigera single nucleopolyhedrovirus; *B. mori*, Bombyx mori; BV, budded virus; ODV, occlusion-derived virus; OB, occlusion body; LD_{50}, 50% lethal dose; LT_{50}, 50% lethal time; SEM, scanning electron microscopy; TEM, transmission electron microscopy; h p.t., hours post transfection; h p.i., hours post infection; PBS, phosphate-buffered saline; SDS-PAGE, SDS-polyacrylamide gel electrophoresis

* Corresponding author.
E-mail address: wuxiaofeng@zju.edu.cn (X. Wu).

https://doi.org/10.1016/j.virol.2018.10.008
Received 11 September 2018; Received in revised form 9 October 2018; Accepted 9 October 2018
Available online 17 October 2018
0042-6822/

In addition to GP64, F protein homologues (F-like proteins) were also identified in group I NPVs, including Autographa californica multiple nucleopolyhedrovirus (AcMNPV), Bombyx mori nucleopolyhedrovirus (BmNPV) and Orgyia pseudotsugata multiple nucleopolyhedrovirus (OpMNPV). It is intriguing that both AcMNPV and OpMNPV F homologues Ac23 and Op21 have no detectable membrane fusion activity, and devoid of the conserved region containing the furin-like cleavage site (Pearson et al., 2001; Rohrmann and Karplus, 2001). Characterization of *Ac23*-null mutant AcMNPV showed that Ac23 is a virulence factor not only in vivo but also in vitro (Lung et al., 2003; Wang et al., 2008; Yu et al., 2009). The previous results suggested that the F-like proteins in group I NPVs probably play a different role from that of GP64.

Since it is hypothesized that the presence of F homologues exerts a positive impact on viral infection, we therefore investigated the biological role of the F-like protein (Bm14) in the infection cycle of Bombyx mori nucleopolyhedrovirus (BmNPV), a significant pathogen in the sericulture industry yet understudied. We utilized a RecE/RecT (ET) homologous recombination system to delete the *Bm14* gene from the BmNPV genome and examined the effects of its deletion on viral infection. Consequently, our results indicated that *Bm14* null reduced infectivity of BV in cell culture to certain extent. In addition, the deletion of *Bm14* was found to extend the time to kill larvae and produce less OBs with a pitted surface and reduced number of embedded ODVs. Western blots clearly indicated that Bm14 is both a component of envelope of BV and ODV. Taken together, our results indicated that *Bm14* plays an important role in regulating the infectivity of BV in vitro and ODV in vivo, the morphogenesis and production of OBs and ODV occlusion.

2. Materials and methods

2.1. Insects, cell lines,viruses and antibodies

The BmN insect cell line was cultured at 27 °C in TC-100 insect medium (PanReac AppliChem) supplemented with 10% fetal bovine serum (Invitrogen Life Technologies), penicillin (100 μg/ml) and streptomycin (30 μg/ml). The BmBacmid was extracted from *E. coli* strain BW25113 and used as template. Viruses were amplified and purified from BmN cells transfected with the bacmid. The T3 strain of BmNPV was used as the WT virus. Larvae of *Bombyx mori* (*B. mori*) were reared on mulberry leaves at 28 °C. Anti-Polh and anti-VP39 antibodies were kindly provided by Prof. Minhui Pan (Southwest University, Chongqing, China).

2.2. Construction of the Bm14 knockout BmNPV bacmid

A *Bm14* knockout BmNPV bacmid was generated via RecE/RecT (ET) homologous recombination as previously described (Kim and Cho, 2005; Yu et al., 2000; Yuan et al., 2008). A linear *CAT* cassette was generated containing the chloramphenicol acetyltransferase gene (*CAT*) flanked by 50 nt fragments homologous to the 5' and 3' regions of the *Bm14* ORF to mediate the insertion of the *CAT* gene into the *Bm14* locus while concomitantly deleting the *Bm14* ORF. The primer pair, Bm14KO-F/Bm14KO-R (Table 1), was used to amplified the *CAT* cassette from plasmid pKD3. The PCR fragment was gel purified and electroporated into *E. coli* BW25113 competent cells harboring the BmNPV bacmid and the temperature sensitive plasmid pKD46. Transformants were plated onto LB agar containing kanamycin and chloramphenicol. The putative *Bm14* knockout colonies grown on the plate were selected and screened by PCR to confirm the absence of the *Bm14* ORF. The PCR screening strategy is outlined in Fig. 1 and the primers used are listed in Table 1. The resulting *Bm14* knockout bacmid was designated bBm^{Bm14KO}.

2.3. Construction of the Bm14 knockout, the repair, and wild-type BmNPV bacmids containing polyhedrin or gfp

To facilitate the visualization of viral infection, *polyhedrin* (*polh*) and *enhanced green fluorescence protein* (*gfp*) was inserted into the *polh* locus simultaneously or individually via Tn7-mediated transposition, as previously described (Shen et al., 2018; Xiang et al., 2013).

To generate the *Bm14* repair bacmid tagged with Flag in the C terminal region, a donor plasmid (pFB1-Bm14Flag-PH-GFP, pFB1-Bm14Flag-PH, or pFB1-Bm14Flag) containing the *Bm14* native promoter was constructed. The gene fragment was PCR amplified from the BmNPV bacmid using the primer pair Bm14RepFlag-F and Bm14RepFlag-R (Table 1). PCR products were digested with the corresponding restriction enzymes and cloned into the transfer plasmids.

The pFB1-Bm14Flag-PH-GFP, pFB1-Bm14Flag-PH or pFB1-Bm14Flag construct was transformed into electrocompetent DH10B cells containing the pMON7124 helper plasmid and the bBm^{Bm14KO} to generate the *Bm14* repair bacmid, *Bm14*RepFlag^{PH-GFP}, *Bm14*RepFlag^{PH} and *Bm14*RepFlag respectively. In addition, the pFB1-PH-GFP plasmid was transformed into DH10B cells containing the pMON7124 helper plasmid and the bBm^{Bm14KO} or BmNPV genome to generate the *Bm14* knockout bacmid (*Bm14*KO^{PH-GFP}) or the positive control bacmid (*Bm*WT^{PH-GFP}), respectively.

Similarly, *Bm14*KO^{PH} and *Bm*WT^{PH} expressing *polyhedrin* were constructed by the transformation of the pFB1-PH plasmid into DH10B cells.

2.4. Analysis of viral growth curve

BmN cells (10^6cells/35 mm-diameter dish) were infected in triplicate with *Bm*WT^{PH-GFP}, *Bm14*KO^{PH-GFP} or *Bm14*RepFlag^{PH-GFP} at an MOI of 10. At the given times points, supernatants containing the BV were harvested, and cell debris was removed by centrifugation at 5000 rpm for 5 min. The titers of BV were determined by $TCID_{50}$ end-point dilution assay in BmN cells (O'Reilly et al., 1992).

2.5. qRT-PCR

BmN cells (10^6cells/35 mm-diameter dish) were infected with *Bm*WT^{PH}, *Bm14*KO^{PH} or *Bm14*RepFlag^{PH} at an MOI of 10. At the indicated time points, the cells were harvested and total RNA was extracted using RNAiso Plus (Takara). First-strand cDNAs were synthesized from 5 μg of total RNA by TransScript One-Step gDNA Removal and cDNA Synthesis SuperMix (TransGen Biotech). qRT-PCR was performed with primer pairs shown in Table 1, as described above.

2.6. Western blot analysis

To detect the expression of Flag-tagged Bm14 protein, BmN cells (10^6cells/35 mm-diameter dish) were infected with *Bm14*RepFlag at an MOI of 10. At the designated time points, the cells were harvested and lysed in cell lysis buffer [20 mM Tris PH7.5, 150 mM NaCl, 1% Triton X-100, 2.5 mM sodium pyrophosphate, 1 mM EDTA, 1% Na_3VO_4, 0.5 μg/ml leupeptin, 1 mM phenylmethanesulfonyl fluoride (PMSF)] (Beyotime) for 30 min on ice. The lysates were mixed with equal volume of 2 × protein loading buffer (Beyotime) and boiled for 7 min. Samples were subjected to SDS-polyacrylamide gel electrophoresis (PAGE) and examined by Western blot with rabbit monoclonal anti-Flag antibody (Cell Signaling Technology).

To examine the effect of *Bm14* deletion on the expression of polyhedrin, BmN cells were infected with *Bm*WT^{PH} or *Bm14*KO^{PH} at an MOI of 10. At various indicated time points, cells were harvested and lysed. The protein concentration in lysates were measured by using BCA Protein Assay Kit (Takara). Next, 20 μg protein samples were mixed with 2 × protein loading buffer (Beyotime) and subjected to western blot. Alpha-tubulin was served as an internal reference.

Table 1
The primers used in this study.

Applications	Primers	Sequences (5′-3′)
Amplification of the *CAT* cassette with flanking sequences	Bm14KO-F	ATAAGCCGTACATGTTGGCTTGCTAATTCAGTCAATATCAGACGTTTATCTAAGTGTAGGCTGGAGCTGCTTC
	Bm14KO-R	ATTTTAATTATACATGTTTTATTTTATTCTTTCAATAATCATAGGATACACATATGAATATCCTCCTTAG
Amplification of *Bm14* with its native promoter	Bm14RepFlag-F	CGGAATTCGATATCGCGTAGAGTGCGT
	Bm14RepFlag-R	ACGCGTCGACTTACTTATCGTCGTCATCCTTGTAATCTTTTATTCTTTCAATAATC
Identification of *Bm14*KO constructs	U-F	CTTTGAAACGGGCGAATGTGAC
	D-R	CCAGCGGTTTACGATGCATTC
	CAT-F	GCTCATGGAAAACGGTGTAAC
	CAT-R	ATGGCAATGAAAGACGGTGA
qRT-PCR analysis of *Bm14*	qRT-Bm14-F	ACGGTGTCATCAATCAAATAACG
	qRT-Bm14-R	TGGCATATCATCGCTATCATCG
qRT-PCR analysis of *Polh*	qRT-Polh-F	GAACAAGAGGAGAAGCAATG
	qRT-Polh-R	TCCAGTTGGCGATTAACTTC
qRT-PCR analysis of *28S rRNA*	qRT-28S rRNA-F	CGACGTTGCTTTTTGATCCT
	qRT-28S rRNA-R	GCAACGACAAGCCATCAGTA

Restriction enzyme sites are underlined. *Eco*RI, GAATTC; *Sal*I, GTCGAC.

2.7. Immunofluorescence

Immunofluorescence assays were performed as described previously with some modifications (Yuan et al., 2011). Briefly, BmN cells on coverslips were infected with *Bm14*RepFLAG at an MOI of 10. At the indicated time points, the cells were fixed in 4% paraformaldehyde, permeabilized in 0.1% TritonX-100, blocked in 0.5%BSA/PBS, and incubated with rabbit monoclonal anti-Flag antibody (1:500, Cell Signaling Technology) overnight. After incubation, the cells subsequently incubated with Alexa 546-conjugated goat anti-rabbit antibody (Invitrogen) at a dilution of 1:500. The cells were then sealed in 4′,6′-diamidino-2-phenylindole (DAPI) (Beyotime), and examined with a ZEISS LSM 780 confocal laser scanning microscopy. As a fluorescent marker of cytoplasmic membrane, 3,3′-dioctadecyloxacarbocyanine perchlorate [DiOC18(3)] (Beyotime) was used when indicated. Images were processed with Zen lite 2012 (Zesis Inc.) and Adobe Photoshop CS (Adobe Systems Inc.). The fluorescence intensity was analyzed using Image J (National Institutes of Health).

2.8. OB production from infected BmN cells

Quantification of occlusion bodies release from cells were performed as described previously (D'Amico et al., 2013). To quantify polyhedra released from infected cells, 2×10^6 BmN cells were infected with *Bm*WT^{PH}, *Bm14*KO^{PH} or *Bm14*RepFlag^{PH} at an MOI of 10. At 168 h p.i., occlusion bodies released from cells were collected from the medium and the unlysed cells were sonicated. Next the pellets were washed twice with 0.1% sodium dodecyl sulfate and once with 0.1 M NaCl and finally resuspended in double-distilled water. The number of occlusion bodies was quantified using a bacterial counting chamber.

2.9. OB purification and DNA extraction

OBs were collected and isolated from the infected larvae. Briefly, 10 μl BV supernatant of *Bm*WT^{PH}, *Bm14*KO^{PH}, or *Bm14*RepFlag^{PH} was injected into the haemocoel of fifth-instar *B. mori* larvae with a micro injector. The OBs were purified from homogenized infected cadavers by differential centrifugation followed by sucrose density gradient ultracentrifugation as described previously (Peng et al., 2011).

Virions were lysed and released from 5×10^8 OBs by incubating with 100 μl of 0.5 M Na_2CO_3 and 50 μl of 10% sodium dodecyl sulfate in a final volume of 500 μl for 10 min at 60 °C. Undissolved debris were removed by low-speed centrifugation and the supernatant fraction containing the virions was further treated with 25 μl of proteinase K (20 mg/ml) for 30 min at 50 °C (Simon et al., 2008). Viral DNA was extracted using phenol-chloroform method. The DNA concentration was determined at 260 nm by using Nanodrop (Thermo).

2.10. Infectivity of OBs

In order to determine if the deletion of *Bm14* has any effect on the infectivity of BmNPV in vivo, *per os* bioassays were conducted as previously described (Lung et al., 2003; Wang et al., 2007). To measure the 50% lethal dose (LD_{50}), 10 μl of solution, spiked with 0 (control), 10^3, 10^4, 10^5, 10^6 and 10^7 OBs, respectively, was smeared on a small piece of fresh mulberry leaf with 1.5 cm diameter. Newly molted fourth-instar *B. mori* larvae were administered individually in compartmentalized boxes. Fresh leaves were only supplied when the entire virus inoculated leaf was consumed. Only larvae that completed ingestion within 8 h were further reared at 25 °C. For the determination of 50% lethal time (LT_{50}), newly molted fourth-instar *B. mori* were starved for 6 h and then inoculated with 10^6 OBs. Inoculated larvae were reared individually as described above. Virus-induced mortality was recorded every 24 h until insect death or pupation. Bioassays with 30 larvae per dosage were performed in triplicates. The LD_{50} value was determined using the probit analysis and LT_{50} value was determined using the Kaplan-Meier estimator in the SPSS 20.0 software (IBM).

2.11. In vitro infectivity of ODVs

The mean titer per OB was determined by endpoint assays as described previously (Lynn, 2003; Simon et al., 2008) with minor modifications. Briefly, 5×10^8 OBs were treated for 30 min with DAS buffer (0.1 M Na_2CO_3, 10 mM EDTA, 166 mM NaCl, pH 11) followed by the addition of 500 mM Tris-HCl (pH 7.5) to bring the sample back to near neutrality. This suspension was treated with 0.1 mg/ml trypsin for 2 h followed by filtration through a 0.45 μm filter. The virus sample s were subjected to 10-fold serial dilutions and the titer was determined by $TCID_{50}$ end-point dilution assay in BmN cells. The data obtained were analyzed by the Spearman-Ka¨rber method.

2.12. Electron microscopy

For scanning electron microscopy (SEM), purified OBs (1×10^8 OBs) were fixed, dehydrated and then dried in Hitachi Model HCP-2 critical point dryer. The samples were coated with gold-palladium and observed by Hitachi Model SU8010 SEM. For transmission electron microscopy (TEM), OBs were fixed, dehydrated, infiltrated and embedded. Ultrathin sections were stained and observed by Hitachi Model H-7650 TEM.

To minimize the possible interference of angle deviation caused by sectioning, we conducted in situ lysis to observe ODV numbers within OBs as described previously (Kuang et al., 2017) with minor modification. Briefly, 10 μl of a suspension of 5×10^8 OBs/ml was loaded onto a copper grid and absorbed for 15 min and the remaining solution

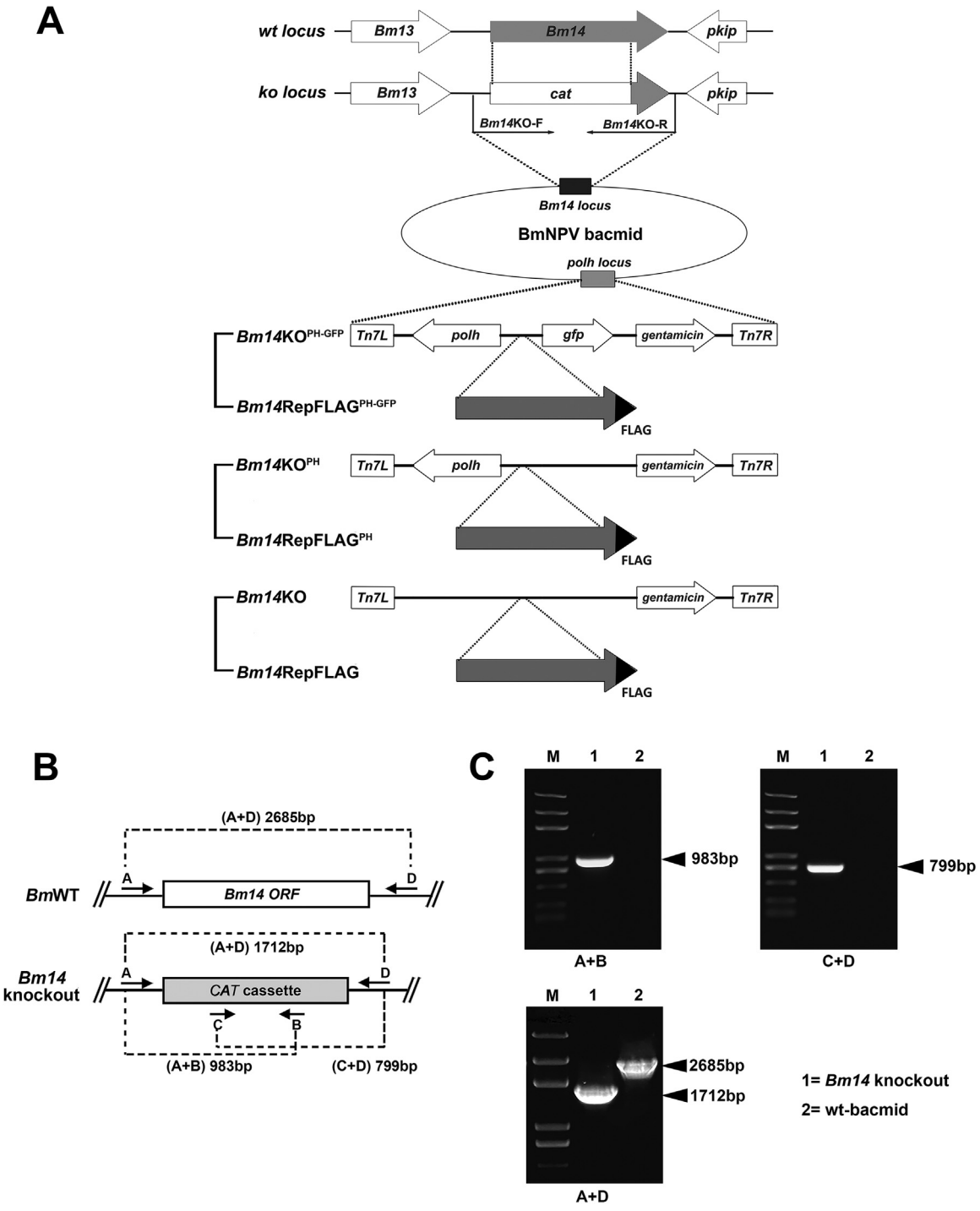

Fig. 1. Construction of recombinant bacmids. (A) Strategy for construction of *Bm14*KO and repair bacmids. The ORF of *Bm14* was replaced by a chloramphenicol acetyltransferase gene (*CAT*) via RecE/RecT (ET) homologous recombination to generate bBm^{Bm14KO}. The lower diagram shows the fragments inserted into the *polh* locus to generate *Bm14*KO^{PH-GFP}, *Bm14*KO^{PH}, *Bm14*RepFlag^{PH-GFP}, *Bm14*RepFlag^{PH} and *Bm14*RepFlag, respectively. (B) Diagrams indicating the relative positions of primers A, B, C, and D (arrows) used for PCR screening of *Bm14* ORF deletion. The top diagram represents a wild-type control bacmid containing the native *Bm14* ORF and the bottom illustrates the organization of a putative *Bm14* knockout bacmid. Dashed lines indicate the expected size of the PCR products amplified from specific primer pairs. Primers A and D are located outside the *Bm14* ORF and primers B and C are specific for the *CAT* cassette. (C) The results of agarose gel electrophoresis showing PCR products generated from primer pairs (A + B), (C + D), and (A + D) using a *Bm14* knockout (lane 1) or WT (lane 2) bacmid as template. The primers used are indicated under each panel and the expected sizes of the respective PCR products are indicated by arrowheads. M indicates DNA marker.

was removed by filter paper. A 10 µl volume of 0.5 × DAS buffer was added to dissolve the OBs for 2 min, followed by neutralization with 500 mM Tris-HCl (pH 7.5). The grid was stained with 2% (wt./vol.) phosphotungstic acid and examined by TEM.

2.13. Purification of BV and ODV and fractionation into envelope and nucleocapsid fractions

The purification of BV and ODV was conducted as described previously (Biswas et al., 2018; Wang et al., 2018) with minor

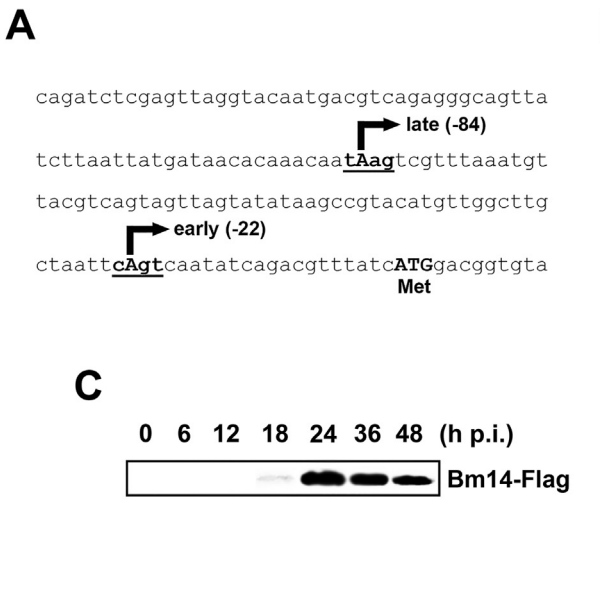

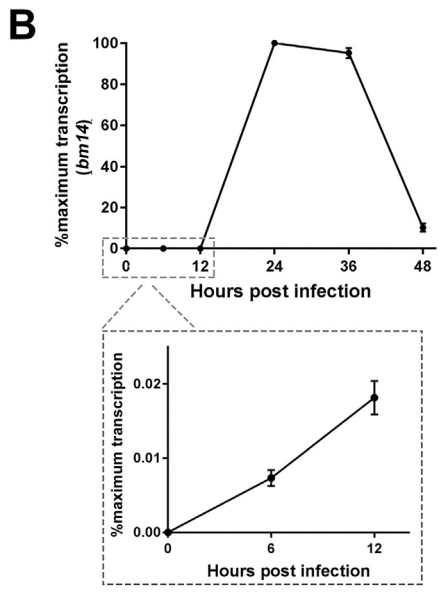

Fig. 2. Temporal expression patterns of Bm14. (A) Transcription start sites of *Bm14* transcripts. A transcriptomic study (Katsuma et al., 2011) revealed that *Bm14* is transcribed from early and late promoters that are 22 and 84 nucleotides upstream of the translation start codon, respectively. (B) Temporal expression of *Bm14* mRNA. BmN cells were infected with *Bm*WT$^{PH\text{-}GFP}$ at an MOI of 10. At various time points, cells were harvested and total RNA was extracted. The cDNA reverse-transcribed from total RNA was subjected to qPCR analysis. Magnified view of the dashed box area is shown below. (C) Temporal expression of the Bm14 protein. BmN cells were infected with *Bm14*RepFlag at an MOI of 10 and harvested at the designated time points, lysed, and subjected to Western blot using an anti-Flag antibody. All assays were carried out in triplicates.

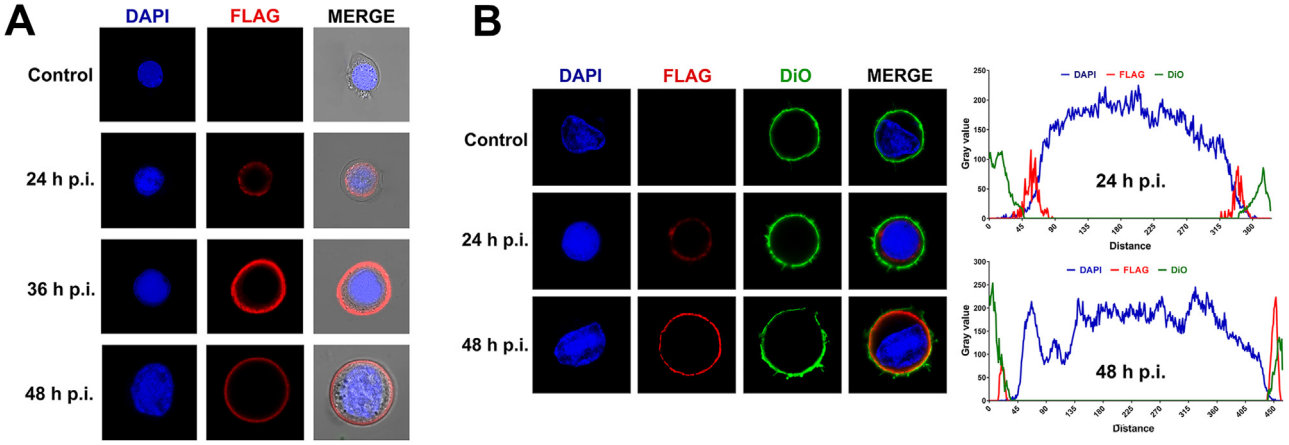

Fig. 3. Subcellular localization of Bm14 protein as demonstrated by immunofluorescence. (A) Immunofluorescence analysis by confocal microscopy. At the indicted time points, the cells infected with *Bm14*RepFLAG were fixed, permeabilized, blocked, and incubated with rabbit anti-FLAG antibody, followed by treatment with AlexaFluor 546-conjugated goat anti-rabbit IgG. DAPI was used for indicating the location of cell nucleus. From left to right: cell nucleus (DAPI; blue), Bm14-FLAG (FLAG; red), and merged images. (B) Colocalization of Bm14 with DiO. At 24 and 48 h p.i., *Bm14*RepFLAG-infected cells were treated as above and stained with DiO, a fluorescent marker of cell membrane, at 27 °C for 15 min. From left to right: cell nucleus (DAPI; blue), Bm14-FLAG (FLAG; red), cell membrane (DiO; green) and merged images. Fluorescent intensity profile of respective channel is shown in the right side.

modifications. For BV purification, haemolymph from the fifth instar *B. mori* larvae orally infected with OBs from *Bm14*RepFlag^{PH} was used to infect BmN cells. At 72 h p.i., the supernatants were harvested and the BV particles were ultracentrifuged with 25% (w/v) sucrose cushion at 20,000 r.p.m. for 90 min, and the pellets were resuspended in PBS supplemented with protease inhibitor cocktail and stored at −80 °C till further use. For ODV purification, the purified OBs (5×10^8 OBs) were firstly heated at 80 °C for 40 min to inactivate endogenous protease, and then lysed with 1 × DAS buffer at 37 °C for 30 min, followed by neutralization with 1/10 vol of Tris-HCl (500 mM, pH 7.5). The supernatants were purified by ultracentrifugation through 30–60% (w/v) sucrose at 20,000 r.p.m. for 90 min, and the multiple bands of ODV from the 40–55% (w/v) sucrose layer were collected and diluted with 10 vol of PBS, followed by further centrifugation at 20,000 r.p.m. for 90 min. The ODV pellets were re-suspended in PBS (with cocktail) and stored at −80 °C for later use. For fractionation of BV and ODV into nucleocapsid and envelope, purified BV or ODV (200 μg) was incubated with the same volume of 2% NP-40 for 30 min at 4 °C and spun at 20,000 r.p.m. for 60 min. The supernatants were collected as envelope fractions, and the nucleocapsid pellets were washed and then resuspended in PBS (with cocktail). Western blot analyses were performed with anti-GP64 (1:5000, Sigma-Aldrich), anti-VP39 (1:5000), and anti-Flag (1:5000, Cell Signaling Technology).

3. Results

3.1. Construction of the Bm14 knockout and repaired BmNPV bacmids

To investigate the function of *Bm14* in the BmNPV infection cycle, the *Bm14* knockout BmNPV bacmid was generated via RecE/RecT (ET) homologous recombination as described previously (Kim and Cho, 2005; Yu et al., 2000; Yuan et al., 2008). The *Bm14* locus was replaced by a chloramphenicol acetyltransferase gene (*CAT*) (Fig. 1A). Bacmid clones isolated after recombination were screened by PCR to determine the successful insertion of the *CAT* cassette into the *Bm14* locus. The PCR screening strategy is outlined in Fig. 1B and the primers used are listed in Table 1. Primers A and D are located outside the *Bm14* ORF and primers B and C are specific for *CAT* cassette. The primer combinations A + B and C + D are expected to generate PCR products of 983 bp and 799 bp, respectively, from successful *Bm14* knockout

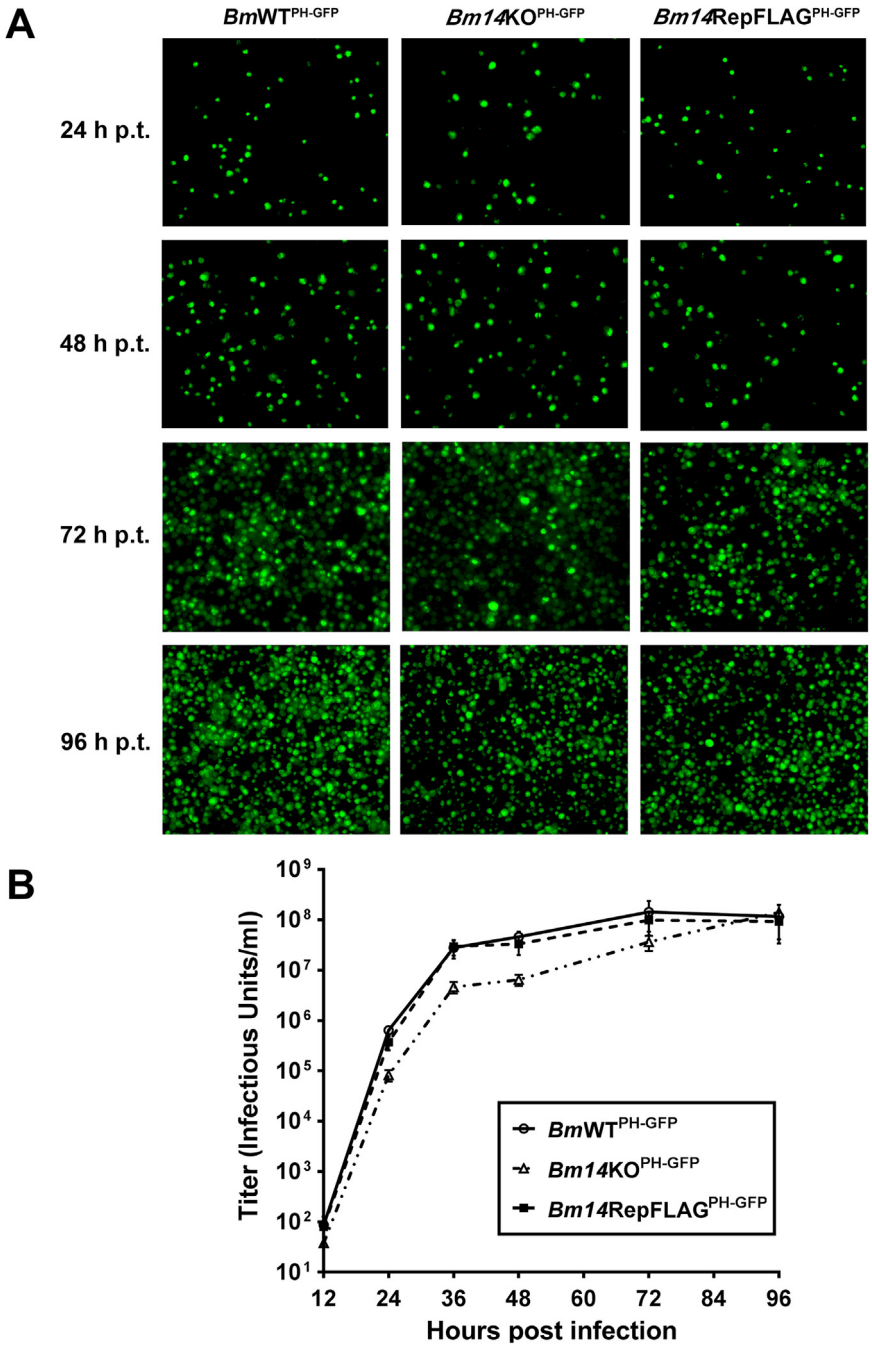

Fig. 4. Analysis of BV production in BmN cells. (A) Microscopy analysis. Fluorescence microscopy revealing the progression of viral infection in BmN cells transfected with *Bm*WT$^{PH\text{-}GFP}$, *Bm14*KO$^{PH\text{-}GFP}$, or *Bm14*RepFlag$^{PH\text{-}GFP}$ from 24 to 96 h p.t. (B) Virus growth curves as determined by $TCID_{50}$ endpoint dilution assays. BmN cells were transfected with individual bacmid DNA and then the supernatants were harvested at the indicated time points. The titers were determined using $TCID_{50}$ endpoint dilution assays. Each data point was determined by three independent assays, and error bars represent standard deviations.

bacmid, but not from wild-type (wt) bacmid (Fig. 1C). In addition, the primer combination A + D would generate the product of 1712 bp from the *Bm14* knockout bacmid, different from those of 2685 bp from the wild-type bacmid. Collectively, the ORF of *Bm14* is successfully disrupted by the *CAT* cassette.

To better monitor the effect of the *Bm14* deletion on viral infection, we introduced the *polyhedrin (polh)* and *enhanced green fluorescence protein* (*gfp*) gene simultaneously or *polh* individually into the *polyhedrin* locus via site-specific transposition to generate *Bm14*KO$^{PH\text{-}GFP}$ and *Bm14*KO^{PH}. To minimize the effects of intrinsic genome on the phenotype resulting from the deletion of *Bm14*, we constructed the repaired bacmids, *Bm14*RepFlag$^{PH\text{-}GFP}$, *Bm14*RepFlag^{PH} and *Bm14*RepFlag, which contained the *Bm14* ORF driven by its native promoter with a Flag-encoding sequence at the C terminus (Fig. 1A). In addition, *Bm*WT$^{PH\text{-}GFP}$ and *Bm*WT^{PH} were also generated as above and acted as the positive controls.

3.2. Temporal pattern of the Bm14 mRNA and protein expression

A previous transcriptomic study showed that *Bm14* mRNA was transcribed from both early and late promoters (Fig. 2A), implying that *Bm14* could be expressed from the early stage of infection. To investigate the accurate expression of *Bm14* mRNA, total RNA was extracted from the *Bm*WT$^{PH\text{-}GFP}$-infected cells at the designated time

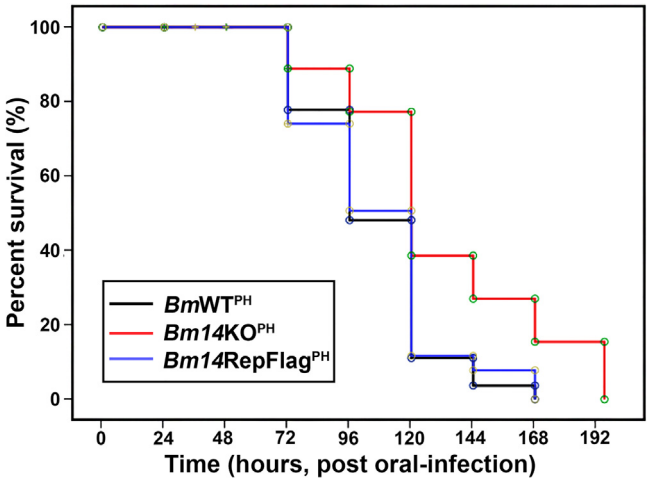

Fig. 5. In vivo analysis of *Bm14* knockout BmNPV. Analysis of the survival time in fourth-instar *B. mori* larvae infected with OBs from *Bm*WT^{PH}, *Bm14*KO^{PH} or *Bm14*RepFlag^{PH}. Survivals percentage of larvae orally infected with 10^6 OBs/larva were plotted against time after oral infection. The LT_{50} of *Bm14*KO^{PH} and *Bm*WT^{PH} were 131 h and 105 h, respectively. No significant differences were detected between *Bm*WT^{PH} and *Bm14*RepFlag^{PH} (106 h). Results shown are determined from the average of three independent experiments.

Table 2
Dose-mortality of *Bm*WT^{PH}, *Bm14*KO^{PH} and *Bm14*RepFlag^{PH} for fourth *B. mori* larve.

Virus	LD_{50} (95% CL) ($\times 10^7$ OB ml^{-1})	Potency ratio (95% CL)[a]
*Bm*WT^{PH}	1.544 (0.591–5.938)	
*Bm14*KO^{PH}	7.063 (2.091–42.263)	0.219 (0.037–0.902)
*Bm14*RepFlag^{PH}	1.287 (0.506–4.759)	1.200 (0.332–4.575)

[a] The potency ratio was calculated by dividing the LD_{50} of by *Bm14*KO^{PH} or *Bm14*RepFlag^{PH} that of *Bm*WT^{PH}. Significant difference was based on whether the 95% confidence limit (CL) of the potency ratio included the value of 1.0.

Table 3
Time-mortality of *Bm*WT^{PH}, *Bm14*KO^{PH} and *Bm14*RepFlag^{PH} for fourth *B. mori* larve.

Virus	LT_{50} (h)	95% Fiducial limit (h)	
		Lower	Upper
*Bm*WT^{PH}	105.78	96.29	115.26
*Bm14*KO^{PH}	131.83	117.29	146.35
*Bm14*RepFlag^{PH}	106.62	95.93	117.31

points and reverse-transcribed cDNA was subjected to qPCR analysis, using 28S rRNA as internal control. Results revealed that the *Bm14* transcript was firstly detected at 6 h p.i., then rapidly increased during 12 and 24 h post infection (p.i.), reaching a peak at 24 h p.i. (Fig. 2B). Next, we investigated the expression pattern of Bm14 protein. Time-course analysis showed that Bm14 protein was initially expressed at 18 h p.i. at a low level, and the subsequent pattern was consistent with that of *Bm14* mRNA (Fig. 2C). Taken together, *Bm14* is an early/late gene which mainly expresses at late and very late stage of viral infection.

3.3. Subcellular localization of Bm14 during the viral infection

To further characterize the function of Bm14 in the viral life cycle, the subcellular localization of Bm14 was analyzed using immunofluorescence microscopy. Cells infected with *Bm14*RepFLAG were probed with rabbit monoclonal anti-FLAG antibody and analyzed by confocal microscopy. In *Bm14*RepFLAG-infected cells, Bm14 was detected in the periphery of nuclear membrane at 24 h p.i. By 36 h p.i., the ongoing Bm14 was localized to cytoplasmic membrane with part of Bm14 detected within the cytoplasm. By 48 h p.i., the Bm14 signal was predominantly concentrated at the cytoplasmic membrane (Fig. 3A). To further investigate the precise localization of Bm14, we compared the location of Bm14 with that of the DiO, a fluorescent marker of cytoplasmic membrane. As expected, immunocytochemical analysis revealed that the complete collocation of Bm14 with DiO at 48 h p.i. (Fig. 3B), indicating that Bm14 possibly experiences a set of migration and finally localize to the cytoplasmic membrane during the viral infection cycle. The profile of fluorescence intensity across the cells showed the identical results (Fig. 3B). In combination, these findings suggested that Bm14 exhibited a dynamic distribution throughout the viral infection.

3.4. Bm14 affect the infectivity of BVs

To determine the effect of *Bm14* deletion on BV production, BmN cells were transfected with *Bm*WT$^{PH\text{-}GFP}$, *Bm14*KO$^{PH\text{-}GFP}$ or *Bm14*RepFlag$^{PH\text{-}GFP}$. Transfected cells were observed with fluorescence microscopy. Similar amounts of GFP-positive cells among the three viruses at 24 h post transfection (p.t.) indicated the relatively equal transfection efficiencies among samples. At 96 h p.t., almost all cells were filled with fluorescence signals, implying the generation of infectious BVs (Fig. 4A).

To further investigate the effect of *Bm14* deletion on BV production, analysis of virus growth curve was performed. Briefly, BmN cells were infected with *Bm*WT$^{PH\text{-}GFP}$, *Bm14*KO$^{PH\text{-}GFP}$ or *Bm14*RepFlag$^{PH\text{-}GFP}$ at an MOI of 10, and the BV titers were determined by $TCID_{50}$ endpoint dilution at the indicated time points. As is shown in Fig. 4B, the production of infectious BVs from three BV samples revealed a similar steady increase. However, the titers of *Bm14*-null mutant and control viruses differed (by appropriately 10-fold) from 24 h p.i. (F [Fisher's statistic] = 219.948; df [degree of freedom] = 1; $P < 0.01$) to 72 h p.i. ($F = 26.362$; $df = 2$; $P < 0.01$). It was noticeable that both viruses were in log-phase production of BV at this period of time. By 96 h p.i., BV titers were indistinguishable among the viruses and reached a plateau. Thus, our results indicated that *Bm14* might participate in regulating the production of infectious BVs in cell culture and its deletion may reduce the production rate.

3.5. Bm14 null affected the infectivity for B. mori larvae

The infectivity of *Bm*WT^{PH}, *Bm14*KO^{PH} and *Bm14*RepFlag^{PH} were determined for newly molted fourth-instar *B. mori* larvae in 50% lethal dose (LD_{50}) and 50% lethal time (LT_{50}) bioassays. The data demonstrated that the LD_{50} of larvae infected with *Bm14*KO^{PH} was larger than that of *Bm*WT^{PH} and *Bm14*RepFlag^{PH} infected larvae (Fig. 5; Table 2), and the LT_{50} of *Bm14* knockout mutant was approximately 25 h longer than control virus (Table 3). Statistical analysis showed that there was significant difference in the LD_{50} between *Bm14*-null mutant and control viruses, as evidenced by the 95% confidence interval of the potency ratio not including 1.0. Therefore, our results suggested that *Bm14* might affect the efficiency of oral infection to certain extent.

3.6. Bm14 deletion reduced the production of OBs

To investigate the reason behind delayed larval death in *Bm14* mutants, we firstly examined the production of occlusion bodies as well as the expression level of polyhedrin, the major component of OB. The results revealed that both polyhedrin protein and occlusion bodies showed lower levels at the late stage upon infection with *Bm14*KO^{PH} mutant (Figs. 6A, B, C).

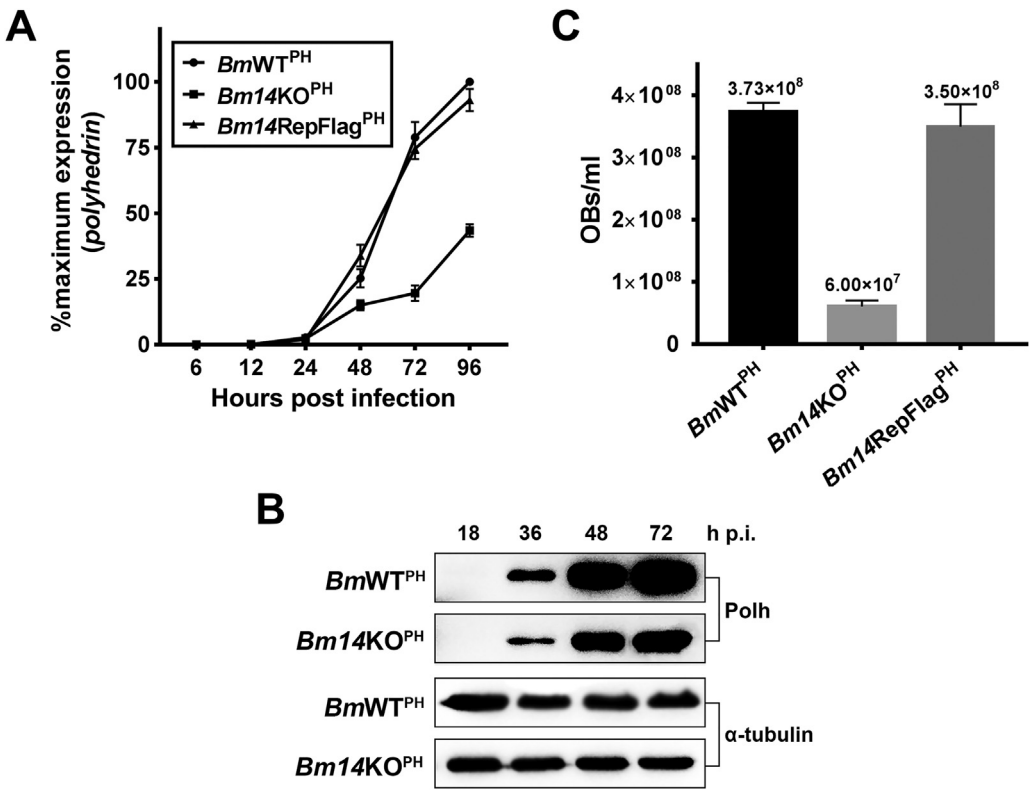

Fig. 6. Effect of *Bm14* null on the expression of polyhedrin and production of OBs. (A, B) Two sets of BmN cells infected with an MOI of 10 was used for total RNA or protein extraction and analyzed by real-time PCR or western blot to determine polyhedrin mRNA and protein levels, respectively. (C) The other set of cells was harvested to quantify polyhedra produced by recombinant viruses. Data shown are means ± SD (n = 3).

3.7. Bm14 knockout impaired OB morphogenesis and generated OBs with reduced embedded ODVs

To investigate whether deletion of *Bm14* affects virus morphogenesis, OBs from the infected larvae were analyzed by scanning electron microscopy (SEM) and transmission electron microscopy (TEM) (Fig. 7A). SEM results showed that wide-type OBs yielded smooth surfaces and sharp edges (Figs. 7a, b), while most OBs produced by *Bm14*-null mutant had pitted surfaces and exhibited a more irregular profile (Figs. 7e, f). When thin sections of OBs were further analyzed using TEM, the numbers of the ODVs appeared to be less than that of the control virus (Figs. 7c, 7g). To avoid possible interference derived from angle of deviation caused by sectioning, OBs were in situ lysed, negatively stained and examined by TEM to determine the absolute number of embedded ODV. As depicted in Figs. 7d and h, the assembly and the number of ODVs within each OB could be clearly observed and the results were consistent with the above.

Next we performed DNA extractions from 5×10^8 OBs and proceeded to Kruskal-Wallis and Mann-Whitney nonparametric analyses. No significant differences in the mean amounts (± standard deviations) of DNA in OBs were detected between the *Bm*WT^{PH} (622.7 ± 15.5 ng/μl) and *Bm14*RepFlag^{PH} (598 ± 14.93 ng/μl). However, *Bm14*-null OBs yielded 45% less DNA, 345 ± 49.9 ng/μl was obtained from 5×10^8 OBs, representing an approximately 1.8-fold reduction in OBs DNA content (Fig. 7B).

Moreover, we also investigated the infectivity of ODVs derived from equal numbers of *Bm*WT^{PH}, *Bm14*KO^{PH} and or *Bm14*RepFlag^{PH} OBs by end point dilution (Fig. 7C). Samples of 5×10^8 OBs of *Bm*WT^{PH} and *Bm14*RepFlag^{PH} produced titers of 1.24×10^7 and 9.69×10^6 infectious units/ml, respectively. In contrast, the same number of OBs of the *Bm14* deletion mutant yielded a titer of 1.66×10^6 infectious units/ml, approximately 7.5 times less infectivity than the control, which indicated the less infectious ODVs within the *Bm14*-null OBs.

3.8. Bm14 is present in the envelope of both BV and ODV

While two proteomic studies of AcMNPV BV (Wang et al., 2010b) and ODV (Braunagel et al., 2003) were reported to identify proteins associated with each virion phenotype, neither study identified Bm14 as an ODV or BV structural protein. To determine the location of Bm14, BV and ODV were purified and analyzed by Western blotting. In addition, the biochemically fractionated envelope and nucleocapsid fractions of the BV and ODV particles were also analyzed. The results indicated that Bm14 is associated with both BV and ODV and localizes to the envelope fraction (Fig. 8). The BV-specific protein envelope GP64 and the major nucleocapsid protein VP39 were used as controls to assess the purity of the samples.

4. Discussion

To determine the biological functions of F-like protein in *gp64*-containing group I NPV (such as BmNPV), we utilized the λ-Red homologous recombination system to delete the *Bm14* gene (Fig. 1). Our results showed that *Bm14* affected the infectivity of BV in vitro and ODV in vivo. In addition, a series of functional analyses, including oral infectivity, OB production and morphology, and ODV occlusion, indicated that *Bm14* plays a distinct role different from that of GP64.

Bioassays performed with *B. mori* larvae revealed the difference in host survival duration. The LT_{50} of *Bm14* knockout virus was approximately 25 h longer than wild-type virus in infected larvae, and it was similar with the results obtained from a previous study, where it was found that host mortality was declined by more than 28% in *T. ni* larvae orally infected by *Ac23*-null mutant (Lung et al., 2003) (Fig. 5, Table 2). Moreover, the deletion of *Bm14* led to an increase of LD_{50} (Table 1). These results suggest that *Bm14* might be involved in efficient infection to the permissive hosts and also imply its role at the organismal level.

Next, we sought to decipher the mechanism by which *Bm14* null delayed the morality of infected larvae. Previously, the deletion of *Ac23* was found to produce smaller OBs and ODVs with fewer nucleocapsids (Yu et al., 2009). In addition, the presence of *Ac23* could promote both

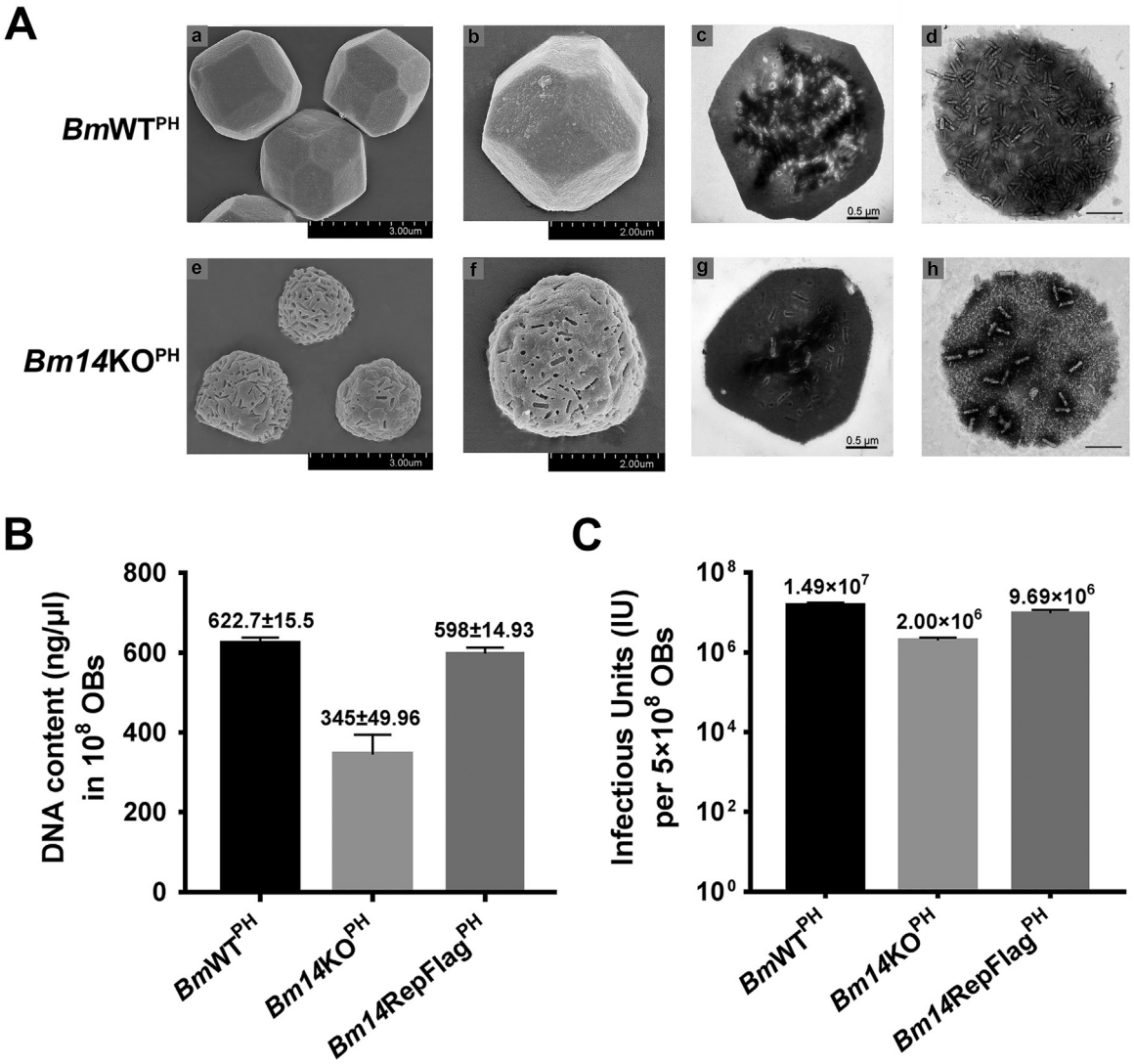

Fig. 7. Electron microscopy analysis of OBs purified from infected larvae and comparison of in vitro infectivity of ODVs. (A) OBs purified from the infected larvae were observed by SEM (a, b, e, f) to assess the surface morphology. TEM analysis of ultrathin sections of OBs (c, g). Negative staining EM showed the ODVs embedded in the lysed OBs (d, h). The corresponding virus names of OBs were indicated on the left. The bars indicate 2 μm or 0.5 μm. (B) Mean amounts of DNA extracted from 5×10^8 OBs of *Bm*WT^{PH}, *Bm14*KO^{PH}, or *Bm14*RepFlag^{PH}. Values above the bars indicate means, and error bars indicate standard deviations. (C) BmN cells were serially infected (10^{-1}–10^{-9}) with ODVs derived from OBs. ODV titers were calculated by endpoint dilution and analyzed by Spearman-Ka¨rber method. Values above bars indicate means.

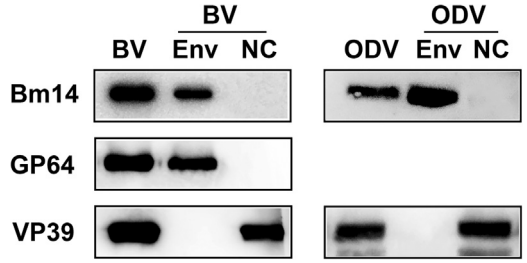

Fig. 8. Western blot analysis of Bm14 in purified and fractionated virions. BV and ODV were purified by differential centrifugation followed by sucrose density gradient ultracentrifugation, and analyzed by Western blotting. The blots were probed individually with an anti-Flag antibody to detect Bm14, anti-AcV5 monoclonal antibody to detect the BV envelope protein GP64, and anti-VP39 to detect the nucleocapsid protein VP39. NC, nucleocapsid fraction; Env, envelope fraction.

the yield and the infectivity of BVs in cell culture (Wang et al., 2008). In this study, additional interesting findings were identified upon *Bm14* mutation. Focusing on the very late gene *polh*, where hyperexpression occurred at least 24 h p.i., however, at 36 h p.i. and thereafter, *polh* expression of *Bm14*KO mutant-infected cells failed to maintain an efficient increase as those of control virus (Figs. 6A, B). The other very late gene *p10* also showed similar expression pattern (data not shown). As the major component of OBs, the reduced expression of *polh* led to the decrease of OB production (Fig. 6C). Furthermore, SEM and TEM showed that while the OBs of control viruses had a smooth surface and sharp profiles, the mutant had a pitted surface, and the number of ODVs was markedly lower than those of the control virus (Fig. 7A), which was consistent with a lower viral DNA content (Fig. 7B). The rod shaped pits on the surface of mutant OBs appear to be the loss of virion bundles. Similar phenomenon was found in the mutant lacking the *p10*, *PEP*, *Ac78* or *P33* gene (Gross et al., 1994; Kuang et al., 2017; Vlak et al., 1988; Williams et al., 1989). P33 is a flavin adenine dinucleotide (FAD)-linked sulfhydryl oxidase essential for BV production and multiply enveloped ODV formation (Kuang et al., 2017; Long et al., 2009;

Wu and Passarelli, 2010). The sulfhydryl oxidase activity has also been suggested to be the protection of cells against oxidative stress induced by apoptosis (Morel et al., 2007; Thirunavukkarasu et al., 2008). In a previous study (Santos et al., 2010), *Bm14* was considered to likely participate in stress response under viral infection. This seems to be consistent with the results that *Bm14*-null mutants had reduced cellular ROS levels induced by virus infection and Bm14 was verified to interact with calreticulin (CRT), a host factor regulating apoptosis (data not shown). It is interesting to investigate further whether Bm14 is involved in regulating virus-induced apoptosis, thus affecting the expression of very late genes and OB production. *Ac78* is a core gene associated with ODV envelope (Garavaglia et al., 2012). The homolog of *Ac78* in *Helicoverpa armigera* single nucleopolyhedrovirus (HearNPV) affected the occlusion of ODVs into polyhera and interacted with P33 (Huang et al., 2014; Tao et al., 2013). P10 and PP34 (PEP) are closely related with the morphogenesis and stability of OBs. The previous studies have reported that OBs produced by *p10*-null or *pp34*-null mutant also exhibited ragged surfaces and irregular shapes. Considering the various roles that P10 play during infection ranging from the morphogenesis of OB to affecting the rate of cellular and nuclear lysis during the final stages of the virus replication cycle (Carpentier and King, 2009), we surmise that *Bm14* might affect the formation of large fibrillar structures mediated by P10 (Carpentier et al., 2008; Patmanidi et al., 2003) in the cytoplasm and nuclei of infected cells, and further impair the morphogenesis and stability of OBs, resulting in the failure of ODV occlusion into OBs and the escape of virions from the pitted surface of OBs. Altogether, the relationships between *Bm14* and genes aforementioned deem further investigation.

It was uncertain whether F-like protein of BmNPV was a BV or ODV structural protein. In the present study, Western blot analysis firstly showed that Bm14 is an envelope component of both BV and ODV (Fig. 8). This result was consistent with earlier study on the location of Ac23 in each virion phenotype. To date, only a small number of proteins has been reported to be associated with both the envelopes of BV and ODV from AcMNPV, including Ac16 (BV/ODV-E26), Ac23 (F-like), Ac76, Ac94 (ODV-E25), Ac143 (ODV-E18) and Ac148 (ODV-E56) (Blissard and Theilmann, 2018). The presence of Bm14 on budded virions suggested that it may play a role in virus budding or production of infectious virions, which appeared to corroborate its contribution to the infectivity of BV (Fig. 4B). However, the lack of detectable fusion activity determines that *Bm14* seems unlikely to play an equally important role as GP64 and may be an accessory protein. In addition, subcellular localization analysis by immunofluorescence assays revealed that Bm14 exhibited a dynamic distribution throughout the viral infection from the nuclear membrane to cytoplasmic membrane(Fig. 3). The perinuclear location seems to be consistent with *Bm14* involvement in ODV envelopment and occlusion since ODV envelopes are speculated to be derived from either the inner nuclear membrane (INM) or by de novo synthesis (Braunagel and Summers, 2007; Shi et al., 2015). Moreover, a previous mass spectrometry study showed that ubiquitination modification sites were identified in AcMNPV envelope proteins GP64 and F-like protein (Biswas et al., 2018). Homology comparison revealed the presence of corresponding sites within Bm14. Hence, we surmised that *Bm14* might play distinct roles in both BV and ODV, and different post-translational modifications are likely to determine the destined sites of *Bm14*, that is, either to the INM or to the cytoplasmic membrane via the secretory signals, respectively.

It is well known that the infection cycle of baculoviruses begins with midgut epithelial cells infection. To mediate this infection, the ODV envelope contains an array of *per os* infectivity factors (PIFs), which are essential for the process. In the present study, *Bm14* null mutant was found to produce less infectious ODVs retaining within OBs (Fig. 7C), suggesting that *Bm14* deletion affects the efficiency of oral infection of ODVs. However, it is unlikely to have roles as equally important as that of PIFs. In addition, considering the location of Bm14 in ODV envelope, we speculate that *Bm14* might participate in regulating the primary infection steps mediated by PIFs. Further studies are required to support this speculation.

Taken together, our results collectively support that *Bm14* affects viral infectivity in vitro and in vivo, and is involved in regulating the morphogenesis and production of OBs and ODV occlusion.

Acknowledgments

We acknowledge Associate Professor Lijian Luo (Zhejiang University) for reviewing the manuscript, and we also thank Professor Zhihong Hu (Wuhan Institute of Virology, Chinese Academy of Sciences, Wuhan, China), Professor Kai Yang (Sun Yat-sen University, Guangzhou, China) and Associate Professor Manli Wang (Wuhan Institute of Virology, Chinese Academy of Sciences, Wuhan, China) for suggestions on manuscript. We are also grateful to Dr. Yimeng Li, Dr. Xi Wang, Dr. Wenhua Kuang and Dr. Fengqiao Zhou for help and advice with experimental methods in virion purification and bioassays, and Bio-ultrastructure analysis Lab of Analysis Center in Zhejiang University for technical assistance.

This work was supported by the National Natural Science Foundation of China (project 31772675 and 31472146).

Author contributions

W.X. and X.W. conceived and designed the experiments; W.X., Y.F., H.W. and M.F. performed the experiments; W.X. analyzed the data; Y.F., H.W. and M.F. contributed reagents/materials; W.X. wrote the paper.

Conflicts of interest

The authors declare no conflict of interest. The funding sponsors had no role in the design of the study; in the collection, analyses, or interpretation of data; in the writing of the manuscript, and in the decision to publish the results.

References

Biswas, S., Willis, L.G., Fang, M., Nie, Y., Theilmann, D.A., 2018. Autographa californica nucleopolyhedrovirus AC141 (Exon0), a potential E3 Ubiquitin Ligase, interacts with viral ubiquitin and AC66 to facilitate nucleocapsid egress. J. Virol. 92.

Blissard, G., Black, B., Crook, N., Keddie, B., Possee, R., Rohrmann, G., Theilmann, D., Volkman, L., 2002. Baculoviridae: taxonomic structure and properties of the family, p195-p202. MHV Van Regenmortel et al.

Blissard, G.W., Theilmann, D.A., 2018. Baculovirus entry and egress from insect cells. Annu. Rev. Virol.

Blissard, G.W., Wenz, J.R., 1992a. Baculovirus gp64 envelope glycoprotein is sufficient to mediate pH-dependent membrane fusion. J. Virol. 66, 6829–6835.

Blissard, G.W., Wenz, J.R., 1992b. Baculovirus gp64 envelope glycoprotein is sufficient to mediate pH-dependent membrane fusion. J. Virol. 66, 6829–6835.

Braunagel, S.C., Russell, W.K., Rosas-Acosta, G., Russell, D.H., Summers, M.D., 2003. Determination of the protein composition of the occlusion-derived virus of autographa californica nucleopolyhedrovirus. Proc. Natl. Acad. Sci. USA 100, 9797–9802.

Braunagel, S.C., Summers, M.D., 2007. Molecular biology of the baculovirus occlusion-derived virus envelope. Curr. Drug Targets 8.

Carpentier, D.C., Griffiths, C.M., King, L.A., 2008. The baculovirus P10 protein of Autographa californica nucleopolyhedrovirus forms two distinct cytoskeletal-like structures and associates with polyhedral occlusion bodies during infection. Virology 371, 278–291.

Carpentier, D.C.J., King, L.A., 2009. The long road to understanding the baculovirus P10 protein. Virol. Sin. 24, 227–242.

Carstens, E.B., 2011. Alphabaculovirus 105–117.

Cory, J.S., Myers, J.H., 2003. The ecology and evolution of insect Baculoviruses [review]. Annu. Rev. Ecol. Evol. Syst. 34, 239–272.

D'Amico, V., Slavicek, J., Podgwaite, J.D., Webb, R., Fuester, R., Peiffer, R.A., 2013. Deletion of v-chiA from a baculovirus reduces horizontal transmission in the field. Appl. Environ. Microb. 79, 4056–4064.

Garavaglia, M.J., Miele, S.A., Iserte, J.A., Belaich, M.N., Ghiringhelli, P.D., 2012. Theac53, ac78, ac101, and ac103 genes are newly discovered core genes in the family Baculoviridae. J. Virol. 86, 12069–12079.

Gross, C.H., Russell, R.L., Rohrmann, G.F., 1994. Orgyia pseudotsugata Baculovirus p10 and polyhedron envelope protein genes: analysis of their relative expression levels and role in polyhedron structure. J. Gen. Virol. 75 (Pt 5), 1115.

Haines, F.J., Griffiths, C.M., Possee, R.D., Hawes, C.R., King, L.A., 2009. Involvement of

lipid rafts and cellular actin in AcMNPV GP64 distribution and virus budding. Virol. Sin. 24, 333–349.
Hefferon, K.L., Oomens, A.G., Monsma, S.A., Finnerty, C.M., Blissard, G.W., 1999a. Host cell receptor binding by Baculovirus GP64 and kinetics of virion entry. Virology 258, 455–468.
Hefferon, K.L., Oomens, A.G.P., Monsma, S.A., Finnerty, C.M., Blissard, G.W., 1999b. Host cell receptor binding by Baculovirus GP64 and kinetics of virion entry. Virology 258, 455–468.
Herniou, E., Luque, T., Chen, X., Vlak, J., Winstanley, D., Cory, J., O'Reilly, D., 2001. Use of whole genome sequence data to infer baculovirus phylogeny. J. Virol. 75, 8117.
Huang, H., Wang, M., Deng, F., Hou, D., Arif, B.M., Wang, H., Hu, Z., 2014. The ha72 core gene of baculovirus is essential for budded virus production and occlusion-derived virus embedding, and amino acid K22 plays an important role in its function. J. Virol. 88, 705–709.
Jehle, J.A., Blissard, G.W., Bonning, B.C., Cory, J.S., Herniou, E.A., Rohrmann, G.F., Theilmann, D.A., Thiem, S.M., Vlak, J.M., 2006. On the classification and nomenclature of baculoviruses: a proposal for revision. Arch. Virol. 151, 1257–1266.
Kadlec, J., Loureiro, S., Abrescia, N.G., Stuart, D.I., Jones, I.M., 2008a. The postfusion structure of baculovirus gp64 supports a unified view of viral fusion machines. Nat. Struct. Mol. Biol. 15, 1024–1030.
Kadlec, J., Loureiro, S., Abrescia, N.G.A., Stuart, D.I., Jones, I.M., 2008b. The postfusion structure of baculovirus gp64 supports a unified view of viral fusion machines. Nat. Struct. Mol. Biol. 15, 1024–1030.
Kataoka, C., Kaname, Y., Taguwa, S., Abe, T., Fukuhara, T., Tani, H., Moriishi, K., Matsuura, Y., 2012. Baculovirus GP64-mediated entry into mammalian cells. J. Virol. 86, 2610–2620.
Katou, Y., Yamada, H., Ikeda, M., Kobayashi, M., 2010. A single amino acid substitution modulates low-pH-triggered membrane fusion of GP64 protein in Autographa californica and Bombyx mori nucleopolyhedroviruses. Virology 404, 204–214.
Katsuma, S., Kang, W., Shini, T., Ohishi, K., Kadota, K., Kohara, Y., Shimada, T., 2011. Mass identification of transcriptional units expressed from the Bombyx mori nucleopolyhedrovirus genome. J. Gen. Virol. 92, 200.
Kim, S.Y., Cho, J.Y., 2005. A modified PCR-directed gene replacements method using λ-red recombination functions in Escherichia coli. J. Microbiol. Biotechnol. 15, 1346–1352.
Kingsley, D.H., Behbahani, A., Rashtian, A., Blissard, G.W., Zimmerberg, J., 1999. A discrete stage of baculovirus GP64-mediated membrane fusion. Mol. Biol. Cell 10, 4191.
Kuang, W., Zhang, H., Wang, M., Zhou, N.Y., Deng, F., Wang, H., Gong, P., Hu, Z., 2017. Three conserved regions in Baculovirus sulfhydryl oxidase P33 are critical for enzymatic activity and function. J. Virol. 91.
Li, Z., Blissard, G.W., 2009. The pre-transmembrane domain of the Autographa californica multicapsid nucleopolyhedrovirus GP64 protein is critical for membrane fusion and virus infectivity. J. Virol. 83, 10993–11004.
Li, Z., Blissard, G.W., 2010. Baculovirus GP64 disulfide bonds: the intermolecular disulfide bond of Autographa californica multicapsid nucleopolyhedrovirus GP64 is not essential for membrane fusion and virion budding. J. Virol. 84, 8584–8595.
Long, C.M., Rohrmann, G.F., Merrill, G.F., 2009. The conserved baculovirus proteinp33 (Ac92) is a flavin adenine dinucleotide-linked sulfhydryl oxidase. Virology 388, 231–235.
Lung, O., Westenberg, M., Vlak, J.M., Zuidema, D., Blissard, G.W., 2002. Pseudotyping autographa californica multicapsid nucleopolyhedrovirus (AcMNPV): F proteins from group II NPVs are functionally analogous to AcMNPV GP64. J. Virol. 76, 5729–5736.
Lung, O.Y., Cruzalvarez, M., Blissard, G.W., 2003. Ac23, an envelope fusion protein homolog in the baculovirus Autographa californica multicapsid nucleopolyhedrovirus, is a viral pathogenicity factor. J. Virol. 77, 328–339.
Lynn, D.E., 2003. Comparative susceptibilities of insect cell lines to infection by the occlusion-body derived phenotype of baculoviruses. J. Invertebr. Pathol. 83, 215–222.
Morel, C., Adami, P., Musard, J.F., Duval, D., Radom, J., Jouvenot, M., 2007. Involvement of sulfhydryl oxidase QSOX1 in the protection of cells against oxidative stress-induced apoptosis. Exp. Cell Res. 313, 3971–3982.
Moscardi, F., 1999. Assessment of the application of baculoviruses for control of Lepidoptera. Annu. Rev. Entomol. 44, 257.
O'Reilly, D.R., Miller, L.K., Luckow, V.A., 1992. Baculovirus expression vectors: a laboratory manual. Baculovirus Expr. Vectors A Lab. Man.
Oomens, A.G., Blissard, G.W., 1999. Requirement for GP64 to drive efficient budding of Autographa californica multicapsid nucleopolyhedrovirus. Virology 254, 297–314.
Patmanidi, A.L., Possee, R.D., King, L.A., 2003. Formation of P10 tubular structures during AcMNPV infection depends on the integrity of host-cell microtubules. Virology 317, 308–320.
Pearson, M.N., Russell, R.L., Rohrmann, G.F., 2001. Characterization of a baculovirus-encoded protein that is associated with infected-cell membranes and budded virions. Virology 291, 22–31.
Peng, K., van Lent, J.W., Vlak, J.M., Hu, Z., van Oers, M.M., 2011. In situ cleavage of baculovirus occlusion-derived virus receptor binding protein P74 in the peroral infectivity complex. J. Virol. 85, 10710–10718.
Plemper, R.K., 2011. Cell entry of enveloped viruses. Curr. Opin. Virol. 1, 92–100.
Rohrmann, G.F., 2011. Baculovirus Molecular Biology.
Rohrmann, G.F., Karplus, P.A., 2001. Relatedness of baculovirus and gypsy retrotransposon envelope proteins. Bmc Evolut. Biol. 1, 1–9.
Santos, S.A., Silva, J.L., Balani, V.A., Seixas, F.A., Fernandez, M.A., 2010. Conserved baculoviral ORFs 10 and 14 from Bombyx mori multiple nucleopolyhedrovirus. Genet. Mol. Res.: GMR 9, 457–470.
Shen, Y., Wang, H., Xu, W., Wu, X., 2018. Bombyx mori nucleopolyhedrovirus orf133 and orf134 are involved in the embedding of occlusion-derived viruses into polyhedra. J. Gen. Virol.
Shi, Y., Li, K., Tang, P., Li, Y., Zhou, Q., Yang, K., Zhang, Q., 2015. Three-dimensional visualization of the Autographa californica multiple nucleopolyhedrovirus occlusion-derived virion envelopment process gives new clues as to its mechanism. Virology 476, 298–303.
Simon, O., Williams, T., Asensio, A.C., Ros, S., Gaya, A., Caballero, P., Possee, R.D., 2008. Sf29 gene of Spodoptera frugiperda multiple nucleopolyhedrovirus is a viral factor that determines the number of virions in occlusion bodies. J. Virol. 82, 7897–7904.
Tao, X.Y., Choi, J.Y., Kim, W.J., Lee, J.H., Liu, Q., Kim, S.E., An, S.B., Lee, S.H., Woo, S.D., Jin, B.R., Je, Y.H., 2013. The Autographa californica multiple nucleopolyhedrovirus ORF78 is essential for budded virus production and general occlusion body formation. J. Virol. 87, 8441–8450.
Thirunavukkarasu, C., Wang, L.F., Harvey, S.A., Watkins, S.C., Chaillet, J.R., Prelich, J., Starzl, T.E., Gandhi, C.R., 2008. Augmenter of liver regeneration: an important intracellular survival factor for hepatocytes. J. Hepatol. 48, 578–588.
Vlak, J.M., Klinkenberg, F.A., Zaal, K.J., Usmany, M., Klinge-Roode, E.C., Geervliet, J.B., Roosien, J., van Lent, J.W., 1988. Functional studies on the p10 gene of Autographa californica nuclear polyhedrosis virus using a recombinant expressing a p10-beta-galactosidase fusion gene. J. Gen. Virol. 69 (Pt 4), 765.
Wang, M., Tan, Y., Yin, F., Deng, F., Vlak, J.M., Hu, Z., Wang, H., 2008. The F-like protein Ac23 enhances the infectivity of the budded virus of gp64-null Autographa californica multinucleocapsid nucleopolyhedrovirus pseudotyped with baculovirus envelope fusion protein F. J. Virol. 82, 9800–9804.
Wang, M., Wang, J., Yin, F., Tan, Y., Deng, F., Chen, X., Jehle, J.A., Vlak, J.M., Hu, Z., Wang, H., 2014. Unraveling the entry mechanism of Baculoviruses and its evolutionary implications. J. Virol. 88, 2301.
Wang, M., Yin, F., Shen, S., Tan, Y., Deng, F., Vlak, J.M., Hu, Z., Wang, H., 2010a. Partial functional rescue of HearNPV infectivity by substitution of F protein with GP64 from AcMNPV. J. Virol. 84, 11505–11514.
Wang, R., Deng, F., Hou, D., Zhao, Y., Guo, L., Wang, H., Hu, Z., 2010b. Proteomics of the Autographa californica nucleopolyhedrovirus budded virions. J. Virol. 84, 7233–7242.
Wang, X., Chen, C., Zhang, N., Li, J., Deng, F., Wang, H., Vlak, J.M., Hu, Z., Wang, M., 2018. The group I alphabaculovirus-specific protein, AC5, is a novel component of the occlusion body but is not associated with ODVs or the PIF complex. J. Gen. Virol. 99, 585–595.
Wang, Y., Wu, W., Li, Z., Yuan, M., Feng, G., Yu, Q., Yang, K., Pang, Y., 2007. ac18 is not essential for the propagation of Autographa californica multiple nucleopolyhedrovirus. Virology 367, 71–81.
Westenberg, M., Uijtdewilligen, P., Vlak, J.M., 2007. Baculovirus envelope fusion proteins F and GP64 exploit distinct receptors to gain entry into cultured insect cells. J. Gen. Virol. 88, 3302.
Westenberg, M., Wang, H., Ijkel, W.F.J., Goldbach, R.W., Vlak, J.M., Zuidema, D., 2002. Furin is involved in Baculovirus envelope fusion protein activation. J. Virol. 76, 178.
Wfj, I., Goldbach, R.W., Jm, B.G.V., Zuidema, D., Westenberg, M., 2000. A novel baculovirus envelope fusion protein with a proprotein convertase cleavage site. Virology 275, 30–41.
Williams, G.V., Rohel, D.Z., Kuzio, J., Faulkner, P., 1989. A cytopathological investigation of Autographa californica nuclear polyhedrosis virus p10 gene function using insertion/deletion mutants. J. Gen. Virol. 70 (Pt 1), 187.
Wu, W., Passarelli, A.L., 2010. Autographa californica multiple nucleopolyhedrovirus Ac92 (ORF92, P33) is required for budded virus production and multiply enveloped occlusion-derived virus formation. J. Virol. 84, 12351–12361.
Xiang, X., Shen, Y., Yang, R., Chen, L., Hu, X., Wu, X., 2013. Bombyx mori nucleopolyhedrovirus BmP95 plays an essential role in budded virus production and nucleocapsid assembly. J. Gen. Virol. 94, 1669–1679.
Yin, F., Wang, M., Tan, Y., Deng, F., Vlak, J.M., Hu, Z., Wang, H., 2013. Betabaculovirus F proteins showed different efficiencies when rescuing the infectivity of gp64-null Autographa californica Nucleopolyhedrovirus. Virology 436, 59–66.
Yu, D., Ellis, H.M., Lee, E.C., Jenkins, N.A., Copeland, N.G., Court, D.L., 2000. An efficient recombination system for chromosome engineering in Escherichia coli. Proc. Natl. Acad. Sci. USA 97, 5978–5983.
Yu, I.L., Bray, D., Lin, Y.C., Lung, O., 2009. Autographa californica multiple Nucleopolyhedrovirus ORF 23 null mutant produces occlusion-derived virions with fewer nucleocapsids. J. Gen. Virol. 90, 1499–1504.
Yuan, M., Huang, Z., Wei, D., Hu, Z., Yang, K., Pang, Y., 2011. Identification of Autographa californica Nucleopolyhedrovirus ac93 as a core gene and its requirement for intranuclear microvesicle formation and nuclear egress of nucleocapsids. J. Virol. 85, 11664–11674.
Yuan, M., Wu, W., Wang, C., Hu, Y., Yang, Z., Pang, Y, K., 2008. A highly conserved baculovirus genep48 (ac103) is essential for BV production and ODV envelopment. Virology 379 (87).
Zhou, J., Blissard, G.W., 2008. Identification of a GP64 subdomain involved in receptor binding by budded virions of the Baculovirus autographica californica multicapsid nucleopolyhedrovirus. J. Virol. 82, 4449–4460.